

6th Annual Postdoctoral Science Symposium

September 8, 2016



Organized by the MD Anderson Postdoctoral Association
Sponsored by The University of Texas MD Anderson Cancer Center
Alumni & Faculty Association and the Office of Postdoctoral Affairs,
a unit of Faculty and Academic Development

THE UNIVERSITY OF TEXAS
MD Anderson
Cancer Center
Making Cancer History®

APSS ABSTRACT BOOKLET

1. Development of caspase-3 sensors for molecular imaging of cell death.....	4
2. Intranasal Administration of Mesenchymal Stem Cells Promotes Recovery from Cognitive Deficits and Neurological Dysfunction Induced by Cisplatin	5
3. CD109 regulates tumor propagation of radio-resistant glioma stem cells.....	6
4. NOTCH1 activation inhibits head and neck squamous cell carcinoma growth by downregulating proto-oncogenes AXL kinase and α -Catulin.	7
5. Silencing of ERK2 reverses EMT and suppresses the CSC phenotype, inhibiting lung metastasis in triple-negative breast cancer.....	8
6. Understanding the Mechanism of Action of ridinilazole, a Novel Treatment for <i>Clostridium difficile</i>	9
7. Gender –Specific Role of Epithelial STAT3 in K-ras Mutant Lung Cancer	10
8. Blocking c-Met-mediated PARP1 phosphorylation enhances anti-tumor effects of PARP inhibitors	11
9. Differential mechanisms of cancer- versus cancer therapy-related fatigue in patients with acute myeloid leukemia.....	13
10. De novo discovery of candidate gene sets for the avian hair cell regeneration.....	14
11. Inhibition of mitochondrial p53 accumulation prevents cisplatin-induced neuropathy.	15
12. Antineoplastic activity of CDK2/9 inhibitor CCT68127 occurs via induced anaphase catastrophe and inhibition of PEA15 phosphorylation in lung cancer	16
13. Role of CDK9 inhibition as a sensitizer to radiation in esophageal adenocarcinoma: <i>in vitro</i> and <i>in vivo</i> efficacy study	17
14. Dissecting the foreign body response to biomaterials by non-linear intravital microscopy	18
15. Limitations of The SHORT TEST OF FUNCTIONAL HEALTH LITERACY IN ADULTS (S-TOFHLA) as a Health Literacy Measure.....	19
16. Affective Modulation of the Late Positive Potential Following Repeated Exposure to Cigarette Cues in Smokers and Never-smokers.....	20
17. A mouse model of neurodegeneration	21
18. 3-D TRACT-SPECIFIC FUNCTIONAL ANALYSIS OF WHITE MATTER INTEGRITY IN ALZHEIMER'S DISEASE	22
19. A Cell-autonomous Mammalian 12-hour Clock Coordinates Metabolic and Stress Rhythms	25
20. A novel method for imaging the pharmacological effects of antibiotic treatment on <i>Clostridium Difficile</i>	26
21. Targeting immunotherapy to metastatic cancers enhancing oncolytic viruses with immune checkpoints modulation.....	27
22. mTORcise: Replicating Exercise Induced Remodeling of the Heart by targeted deletion of Tuberin.....	28
23. <i>In vitro</i> Demonstration of the Channel Activity of an Anion Channelrhodopsin.....	29
24. A Novel Schema to Enhance Data Quality of Patient Safety Event Reports	30
25. HDAC6 Inhibition Effectively reverses Chemotherapy-Induced Peripheral Neuropathy.	31
26. PEA-15 (phosphoprotein enriched in astrocytes) regulates epithelial-mesenchymal transition and invasive behavior through its phosphorylation in triple negative breast cancer.....	32
27. HPRM: Hierarchical Principal Regression Model of Diffusion Tensor Bundle Statistics	33
28. Levetiracetam mitigates doxorubicin-induced DNA and synaptic damage in neurons	34
29. Regulation of exosome secretion in ovarian cancer.....	35
30. Nuclear proteolysis in the regulation of metabolic genes in multiple myeloma	36
31. Loss of the ISG15 protease USP18 mislocalizes and destabilizes KRAS in lung cancer.....	37
32. TBD	39

33.ZMYND8 reads the dual histone mark H3K4me1-H3K14ac to antagonize the expression of metastasis-linked genes.....	40
34. Evolving Spindlin1 Small Molecule Inhibitors Using Protein Microarrays.....	41
35. Neuroanatomical Differences in Speech Perception Ability in Bilingual Children.....	42
36. Adrenergic signaling promotes cervical tumor growth and dissemination.....	43
37. Unique molecular signatures to distinguish immunotherapy responding and resistant cell lines in melanoma.....	44
38. Predicting the clinical outcomes using imaging covariates with missing responses.....	46
39. Modified oncolytic adenovirus, Delta-24-RGDGREAT, as an immunotherapeutic agent for Glioblastoma.....	47
40. Spatial Large-Margin Angle-Based Classifier for Multi-Category Neuroimaging Data.....	48

1. Development of caspase-3 sensors for molecular imaging of cell death.

Brian J. Engel¹, Argentina Ornelas¹, Zhen Lu², Amer M. Najjar³, William P. Tong¹, Robert C. Bast², Steven W. Millward¹

¹Department of Cancer Systems Imaging, The University of Texas MD Anderson Cancer Center, Houston, TX.

²Department of Experimental Therapeutics, The University of Texas MD Anderson Cancer Center, Houston, TX.

³Department of Pediatrics - Research, The University of Texas MD Anderson Cancer Center, Houston, TX.

Regulation of cell death through apoptosis is critical for proper development and homeostasis of multicellular organisms. One of the hallmarks of cancer is the evasion of apoptosis that would normally suppress tumor growth and invasiveness. Apoptosis is generally triggered by either DNA damage or signaling through death receptors. Cell death signals result in the activation of executioner caspases which cleave hundreds of intracellular substrates and commit the cell to apoptotic death. Caspase-3 is a critical executioner caspase activated by both intrinsic and extrinsic signals. The preferred substrate sequence of caspase-3 is Asp-Glu-Val-Asp (DEVD) with cleavage occurring after the C-terminal aspartic acid.

Currently, monitoring of treatment efficacy is limited to non-targeted anatomical imaging of gross tumor volume. The ability to rapidly and non-invasively measure apoptotic cell death during treatment can be used to rationally optimize the choice of chemotherapy and to maximize therapeutic response. In addition, cell death imaging can reveal non-tumor apoptosis, allowing the prediction and avoidance of side-effects prior to clinical presentation.

Fluorescent lead compound, 2MP-VD-AMC, was synthesized based off the caspase-3 irreversible inhibitor M808. 2MP-VD-AMC was exclusively cleaved by caspase-3 as determined by *in vitro* caspase enzyme cleavage assays. Furthermore, cleaved AMC accumulated in cells treated with the pro-apoptotic TRAIL ligand, but not untreated cells. We conjugated a C-terminal propyne to the 2MP-VD scaffold and utilized Cu-catalyzed click chemistry with [¹⁸F]-fluoroethylazide to generate the first generation PET radiotracer, 2MP-VD-MeE[¹⁸F]. 2MP-VD-MeE[¹⁸F] shows strong accumulation in TRAIL treated vs untreated cells. Second generation radiotracers were developed by derivatizing the terminal alkyne followed by click reaction with [¹⁹F]-fluoroethylazide. Substitution of valine for benzyl threonine (2MP-TbD) improved *in vitro* caspase-3 cleavage for both the fluorescent and [¹⁹F] derivatives. Lead candidates 2MP-VD-MeE[¹⁸F] and 2MP-TbD-MeE[¹⁸F] will be used *in vivo* to non-invasively observe cell death in platinum- and taxane-treated ovarian cancer xenografts. In the future, these compounds can provide an immediate pharmacodynamic readout of experimental compound efficacy in animal models of cancer, dramatically accelerating early-phase drug trials and personalizing patient care.

2. Intranasal Administration of Mesenchymal Stem Cells Promotes Recovery from Cognitive Deficits and Neurological Dysfunction Induced by Cisplatin

Gabriel S. Chiu¹, Nabila Boukelmoune¹, Sahar Rizvi¹, Annemieke Kavelaars¹, Cobi J. Heijnen¹

¹Laboratory of Neuroimmunology, Department of Symptom Research, Division of Internal Medicine, University of Texas M.D. Anderson Cancer Center, Houston, TX

Cognitive impairments are common side effects of chemotherapy treatment that may persist after the secession of intervention. Here, we tested the effects of nasal mesenchymal stem cell (MSC) administration on the neurotoxic side effects of cisplatin treatment. Adult C57Bl/6J mice were treated with saline or cisplatin (2.3 mg/kg) for two cycles. One million MSC were administered intranasally at 48h and 96h after the last injection of cisplatin. MSC administration promoted recovery in cognitive function as measured in the novel object/place recognition (NOPR), Y- maze, and the Puzzle Box tests. Additionally, MSC promoted recovery from cisplatin-induced decrease in functional network efficiency as measured in resting state fMRI. Synaptic mitochondrial function was also normalized by MSC treatment as measured in the Seahorse XFe 24 Analyzer. MSC administration after cisplatin treatment promoted doublecortin (DCX)+ cells staining in the subventricular zone (SVZ) and the dentate gyrus (DG) of the hippocampus suggesting increased neurogenesis. Furthermore, MSC promoted recovery from white matter damage as measured by myelin basic protein (MBP)+ fibers. Administration of MSC after chemotherapy treatment promoted recovery from cisplatin-induced cognitive impairment and restored mitochondrial function as well as white matter damage and the loss of DCX+ cells. Our data suggest that treatment with MSC may represent a realistic therapeutic strategy for the prevention of chemotherapy-induced cognitive impairment.

3. CD109 regulates tumor propagation of radio-resistant glioma stem cells

Alessandra Audia¹, Mutsuko Minata², Xing Guo¹, Farah Mukheef¹, Hetshree Patel¹, Ravesanker Ezhilarasan³, Erik Sulman³, Ichiro Nakano², and Krishna P. Bhat¹

Departments of ¹Translational Molecular Pathology and ³Radiation Oncology

UT M.D. Anderson Cancer Center, Houston, TX 77030

Department of ³Neurosurgery, The University of Alabama at Birmingham, Birmingham, AL 35294

Glioblastoma (GBM) is a devastating disease that kills about 18,000 Americans every year. GBM patients are uniformly treated with chemo-radiation, but the tumor invariably recurs and the exact molecular mechanisms driving treatment resistance in GBMs are unknown. Newer molecular targeted therapies including VEGF inhibitors, have failed to extend the dismal (approximately 14.6 month median) survival in GBM. Of the molecular subtypes of GBM, the mesenchymal (MES) subtype is considered most aggressive and we have recently shown that these cells exhibit radio-resistance in a NF- κ B dependent manner. Prospectively identifying the MES subset of radio-resistant, cancer stem cells has been challenging due to a lack of cell surface markers to identify these populations. In this study we discovered CD109 as novel tumor initiation marker for the MES subtype of glioma stem cells. Here we report that exposure of GSCs to ionizing radiation (IR) promotes a persistent transcriptomic and phenotypic shift toward a MES subtype in a CD109-dependent manner. We observed that in both *de novo* and IR-induced MES GSCs, CD109⁺, but not CD109⁻ populations are highly clonogenic *in vitro* and radio-resistant and tumorigenic *in vivo*. In addition, inhibition of CD109 through shRNAs attenuates clonogenicity, tumor propagation and radio-resistance and dramatically inhibits YAP/TAZ signaling in MES GSCs. In support of these results, CD109 is significantly associated with the MES subtype of GBMs, correlates with YAP/TAZ expression, and poorer prognosis of GBM patients.

4. NOTCH1 activation inhibits head and neck squamous cell carcinoma growth by downregulating proto-oncogenes AXL kinase and α -Catulin.

Chenfei Huang¹ and Mitchell Frederick¹.

¹Department of Head and Neck Surgery, University of Texas M.D. Anderson Cancer Center, Houston, TX 77030.

Background: Head and neck squamous cell carcinoma (HNSCC) is the sixth most common malignancy worldwide. To identify new treatment targets or biomarkers that could improve therapy, our group characterized the genomic alterations in HNSCC (1), becoming among the first to discover that *NOTCH1* is one of the most frequently mutated genes in this cancer, suggesting the gene is a tumor suppressor. However, the underlying mechanisms remain unclear. This present study is aimed to systematically compare the phenotypic consequences of NOTCH1 signaling in head and neck cells through targeted expression of doxycycline-inducible active Notch1 protein, and define the downstream targets modulated by NOTCH1 signaling.

Methods: Doxycycline-inducible PJ34 (NOTCH1 wild type) and UM22A (NOTCH1 mutant) cell lines for active Notch1 were generated using the Tet-On 3G expression system (Clontech), and were tested for cell growth using clonogenic assay. Notch1-induced downstream gene expression changes in PJ34 and UM22A cells were examined using RNA-seq and qRT-PCR.

Results: Activation of the NOTCH1 pathway inhibits the *in vitro* growth of both PJ34 and UM22A cells, regardless of whether the NOTCH1 receptor is mutant or wild type. This growth inhibition is frequently accompanied by profound changes in cell morphology and induction of the senescence marker β -galactosidase. Furthermore, RNA-seq data have demonstrated that NOTCH1 regulates nearly two thousand genes, and the top genes modulated are involved in critical cancer associated pathways including proliferation, differentiation, migration, cell adhesion and death. Of particular interest, NOTCH1 activation downregulates the proto-oncogenes AXL and α -Catulin and our experiments demonstrated that diminished expression of these targets on their own leads to a loss of growth capacity both *in vitro* and *in vivo*.

Conclusion: Notch1 functions as a tumor suppressor in HNSCC by downregulating of AXL kinase and α -Catulin.

5. Silencing of ERK2 reverses EMT and suppresses the CSC phenotype, inhibiting lung metastasis in triple-negative breast cancer

Mary Kathryn Pitner¹, Hitomi Saso¹, Richard Larson², Rachel M. Sammons³, Huiqin Chen⁴, Caimiao Wei⁴, Gaurav Chauhan¹, Kimie Kondo¹, Naoto T. Ueno¹, Kevin Dalby³, Bisrat G. Debeb², and Chandra Bartholomeusz¹

¹Section of Translational Breast Cancer Research, Department of Breast Medical Oncology, The University of Texas MD Anderson Cancer Center, Houston, Texas, USA.

²Department of Experimental Radiation Oncology, The University of Texas MD Anderson Cancer Center, Houston, Texas, USA.

³Division of Medicinal Chemistry, The University of Texas at Austin, College of Pharmacy, Austin, TX, USA

⁴Department of Biostatistics, The University of Texas MD Anderson Cancer Center, Houston, Texas, USA.

Triple-negative breast cancer (TNBC) is an aggressive subtype lacking estrogen receptor, progesterone receptor, and HER2 overexpression. Patients with TNBC have a generally poor prognosis due to metastasis, high rates of recurrence, and lack of FDA-approved targeted therapies. We previously showed that patients with high-ERK2-expressing TNBC tumors had a higher risk of death than those with low-ERK2-expressing tumors. Moreover, ERK2 but not ERK1 plays an important role in EMT and is required for acquisition of stem cell-like characteristics. TNBC has a high proportion of cancer stem cells and is linked to EMT, two critical features associated with breast cancer progression, metastasis, and recurrence in patients. The MAPK pathway is activated in TNBC, but the roles of ERK isoforms in tumor progression and metastasis are not well defined. We hypothesized that ERK2 but not ERK1 promotes EMT, the CSC phenotype, and metastasis in TNBC.

Knockdown of ERK2 in SUM149 and BT549 TNBC cells significantly inhibited anchorage-independent colony formation ($p < 0.0001$), inhibited formation of mammospheres ($p = 0.003$), and reduced the CSC population ($CD44^+/CD24^-$) ($p = 0.002$) *in vitro*. This effect correlated with a reduction in migration ($p = 0.0004$) and invasion ($p < 0.0001$). Mice injected via the tail vein with SUM149 shERK2 cells had a significantly lower metastatic burden than control mice ($p = 0.0034$) or mice injected with shERK1 cells ($p = 0.0012$), suggesting that ERK2 is a mediator of metastatic burden. To determine the mechanism by which ERK2 mediates this phenotype, we performed a microarray and compared the gene expression levels between SUM149 cells with ERK2 or ERK1 knockdown or transfection with control shRNA. Analysis of microarray data revealed that global gene expression changes associated with ERK2 knockdown predominantly altered regulation of the EMT pathway. Among the genes with ERK2-knockdown-associated expression change was *EGR1*, an immediate early response transcription factor whose downstream targets affect cell growth and differentiation. *EGR1* is down-regulated 6-fold ($p = 0.00013$) compared to control and shERK1 cells. Knockdown of ERK2, but not ERK1, resulted in significantly lower *EGR1* at both the mRNA and protein levels, validating our microarray data.

Our findings support our hypothesis, indicating that ERK2 promotes EMT and the CSC phenotype through *EGR1* and mediates metastasis in TNBC.

6. Understanding the Mechanism of Action of ridinilazole, a Novel Treatment for *Clostridium difficile*

Eugénie Bassères¹, Bradley T. Endres¹, Mohammed Khaleduzzaman¹, Faranak Miraftabi¹, M. Jahangir Alam¹, Richard Vickers², and Kevin W. Garey¹

¹University of Houston, College of Pharmacy, Houston, Texas.

² Summit Therapeutics, Abington, Oxfordshire, UK.

Background: Ridinilazole is a narrow-spectrum, non-absorbable antimicrobial with targeted activity against *C. difficile* currently undergoing clinical trials. However, the mechanism of action of ridinilazole has not been fully elucidated. The purpose of this study was to assess the pharmacologic activity of ridinilazole and determine a potential mechanism of action.

Methods: Antibiotic killing curves were performed using the epidemic *C. difficile* strain R20291 (BI/Nap1/027 strain) using supra-MIC (4x and 40x) and sub-MIC (0.125x, 0.25x, and 0.5x) concentrations of ridinilazole. Following treatment, *C. difficile* cells were collected for CFU counts, toxin A and B production, and morphologic changes using scanning electron and fluorescent microscopy. Human intestinal cells (Caco-2) were co-incubated with ridinilazole - treated *C. difficile* growth media to determine the effects on host inflammatory response (Interleukin (IL)-8).

Results: Treatment at supra-MIC concentrations of ridinilazole resulted in a significant reduction in vegetative cells over 72 hours (4 log difference, $P<0.01$) compared to controls without effect on spore formation. These results correlated with a 75% and 96% decrease in toxin A and B production, respectively ($P<0.05$, each). At sub-MIC levels (0.5X MIC), toxin A and B production were reduced by 91% ($P<0.01$) and 100% ($P<0.001$), respectively, which resulted in a significant attenuation in inflammatory response as measured by a 74% reduction in IL-8 release compared to controls ($P<0.05$). Sub-MIC (0.5x) treated cells formed filamentous structures and were drastically longer in size than control cells (Figure 1). Following fluorescent-labeling, we determined that the cell septum was not forming in sub-MIC treated cells, yet the DNA was dividing.

Conclusions: Collectively these results suggest that ridinilazole has potent killing effects on *C. difficile* that significantly reduces toxin production and attenuates human inflammatory responses. In tandem, ridinilazole also elicits significant effects on cell division, which likely abrogates these downstream effects. These results support the continued development of ridinilazole for the treatment of CDI.

7. Gender –Specific Role of Epithelial STAT3 in K-ras Mutant Lung Cancer

Mauricio da Silva Caetano¹, Hieu Van¹, Emanuel Bugarin², Amber M. Cumpian¹, Huiyuan Zhang³, Scott E. Evans¹, Ignacio I. Wistuba⁴, Carmen Behrens⁵, David Tweardy⁶, Edwin Ostrin¹, Humam Kadara⁴, Stephanie S. Watowich³, and Seyed Javad Moghaddam¹

¹ Pulmonary Medicine, UT MD Anderson Cancer Center

² Medical Student, Instituto Tecnológico y de Estudios Superiores de Monterrey (Mexico)

³ Immunology, UT MD Anderson Cancer Center;

⁴ Translational Molecular Pathology, UT MD Anderson Cancer Center;

⁵ Thoracic/Head and Neck Medical Oncology, UT MD Anderson Cancer Center;

⁶ Internal Medicine, UT MD Anderson Cancer Center;

Activating mutations of K-ras are one of the most common molecular alterations associated with lung cancer. Using a conditional K-ras mutated lung cancer mouse model (CC-LR) we previously showed that IL-6 blockade reduces tumor cell proliferation, and re-educates K-ras mutant lung microenvironment toward an anti-tumor phenotype. Here we first determined that IL-6 responsive transcription factor STAT3 mRNA level was a significant predictor of poor disease-free survival in KRAS-mutant lung cancer. Then, we generated a lung epithelial specific K-ras mutant/STAT3 conditional knockout mouse (LR/*Stat3*^{D/D}) to study the role of epithelial STAT3 activity in K-ras mutant lung cancer. Interestingly, we observed a surprising gender disparity; lack of epithelial STAT3 in female mice inhibited lung cancer and tumor cell proliferation, whereas in males it promoted lung cancer and tumor cell proliferation. Analysis of inflammatory cells in bronchoalveolar lavage fluids of female LR/*Stat3*^{D/D} mice showed significant reduction in total inflammatory cell number with a major impact on macrophage population. We did not observe significant changes in total inflammatory cell number in male LR/*Stat3*^{D/D} mice but we found an increase in neutrophil population. Gene expression analysis of total lung from female LR/*Stat3*^{D/D} mice showed a significant decrease in CD45 expression and phenotypic changes in lung microenvironment characterized by a significant decrease in expression of pro-tumor inflammatory markers IL-6, IL-17, TGF β , arginase1, with an increase in expression of anti-tumor inflammatory markers IFN γ , and *Gzmb*. On the other hand male LR/*Stat3*^{D/D} showed increase in expression of IL-6, CXCL1 and IDO suggestive of a shift toward a pro-tumor lung microenvironment. Women under hormonal therapy replacement show less incidence of lung cancer. Moreover, it has been shown that estrogen signaling is able to decrease IL-6 transactivation. Therefore, we blocked IL-6 using anti IL-6 antibody in male, and inhibited estrogen signaling in female LR/*Stat3*^{D/D} mice by tamoxifen treatment. These treatments resulted in a decreased tumor number in male, and an increased tumor number in female LR/*Stat3*^{D/D} mice, respectively. Taken together, we conclude that epithelial STAT3 signaling has an essential autocrine and paracrine but gender-specific role in K-ras induced lung tumorigenesis which might be mediated by estrogen/IL-6 signaling axis.

8. Blocking c-Met-mediated PARP1 phosphorylation enhances anti-tumor effects of PARP inhibitors

Yi Du¹, Hirohito Yamaguchi¹, Yongkun Wei¹, Jennifer L. Hsu¹, Hung-Ling Wang², Yi-Hsin Hsu¹, Wan-Chi Lin¹, Wen-Hsuan Yu^{1,3}, Paul G. Leonard^{4,9}, Gilbert R. Lee IV^{4,9}, Mei-Kuang Chen^{1,3}, Katsuya Nakai¹, Ming-Chuan Hsu¹, Chun-Te Chen¹, Ye Sun¹, Yun Wu⁵, Wei-Chao Chang^{2,6}, Wen-Chien Huang⁷, Chien-Liang Liu⁷, Yuan-Ching Chang⁷, Chung-Hsuan Chen⁶, Morag Park⁸, Philip Jones⁹, Gabriel N. Hortobagyi¹⁰, and Mien-Chie Hung^{1,2,3,11*}

¹Department of Molecular and Cellular Oncology, The University of Texas MD Anderson Cancer Center, Houston, TX, USA.

²Graduate Institute of Cancer Biology and Center for Molecular Medicine, China Medical University, Taichung, Taiwan.

³The University of Texas Graduate School of Biomedical Sciences at Houston, Houston, TX, USA.

⁴Department of Genomic Medicine, The University of Texas MD Anderson Cancer Center, Houston, TX, USA.

⁵Department of Pathology, The University of Texas MD Anderson Cancer Center, Houston, TX, USA.

⁶Genomics Research Center, Academia Sinica, Taipei, Taiwan.

⁷Department of Surgery, Mackay Memorial Hospital, Taipei, Taiwan.

⁸Department of Biochemistry, McGill University, Montreal, Quebec, Canada.

⁹Institute for Applied Cancer Science, The University of Texas MD Anderson Cancer Center, Houston, TX, USA.

¹⁰Department of Breast Medical Oncology, The University of Texas MD Anderson Cancer Center, Houston, TX, USA.

¹¹Department of Biotechnology, Asia University, Taichung, Taiwan. ***Correspondence:** Mien-Chie Hung. E-mail: mhung@mdanderson.org

Poly (ADP-ribose) polymerase (PARP) inhibitors have emerged as promising therapeutics for many diseases, including cancer, in clinical trials. One PARP inhibitor, olaparib (Lynparza™, AstraZeneca), was recently approved by the FDA to treat ovarian cancer with *BRCA* mutations. Tumor suppressors *BRCA1* and *BRCA2* play essential roles in repairing DNA damage. Notably, mutations in *BRCA1* and *BRCA2* genes have been associated with increased risk of ovarian and breast cancers and sensitivity to PARP1 inhibition. PARP inhibitors were therefore initially investigated in clinical trials for both ovarian cancer and triple-negative breast cancer (TNBC), as this tumor type can harbor defective *BRCA1* or *BRCA2*. However the discrepant clinical observations of olaparib response in different cohorts raise the important question of how to increase the response rate of TNBC—and other cancer types—to PARP inhibitors. On another hand, increased levels of reactive oxygen species (ROS) in cells can cause oxidative DNA damage that leads to genomic instability and tumor development. ROS-induced DNA damage, such as single-strand breaks, recruits PARP1 to the lesion sites to orchestrate the DNA repair process through poly-ADP-ribosylation (PARylation) of itself and its target proteins, including histone proteins. PARylated histones destabilize the chromatin structure, allowing the DNA repair machinery to access the damaged DNA site. Those background provide a hint whether the molecule which mediates ROS-induced activity of PARP1 may contribute the PARP inhibitor

response. Here we show that receptor tyrosine kinase c-Met associates with and phosphorylates PARP1 at Tyr907 in response to the ROS condition. Phosphorylation of PARP1 Tyr907 increases PARP1 enzymatic activity and reduces binding to a PARP inhibitor, thereby rendering cancer cells resistant to PARP inhibition. Combining c-Met and PARP1 inhibitors synergized to suppress growth of breast cancer cells *in vitro* and xenograft tumor models. Similar synergistic effects were also observed in a lung cancer xenograft tumor model. These results suggest that PARP1 pTyr907 abundance may predict tumor resistance to PARP inhibitors, and that treatment with a combination of c-Met and PARP inhibitors may benefit patients bearing tumors with high c-Met expression who do not respond to PARP inhibition alone.

9. Differential mechanisms of cancer- versus cancer therapy-related fatigue in patients with acute myeloid leukemia

Tamara Lacourt, Ph.D.¹, Annemieke Kavelaars, Ph.D.¹, Samuel Shelburne, M.D. Ph.D.², Dimitrios Kontoyiannis, M.D.², Andrew Futreal, Ph.D.³, Cobi J. Heijnen, Ph.D.¹

¹ Department of Symptom Research; Laboratory of Neuroimmunology, The University of Texas MD Anderson Cancer Center, Houston, TX.

² Department of Infectious Diseases, The University of Texas MD Anderson Cancer Center, Houston, TX.

³ Department of Genomic Medicine, The University of Texas MD Anderson Cancer Center, Houston, TX.

Fatigue is a common, debilitating symptom in patients with acute myeloid leukemia (AML). Several mechanisms of AML-related fatigue have been proposed including inflammation. However, it is unclear whether these mechanisms pertain to *cancer*- or *cancer therapy*-related fatigue. We aimed to identify the relative contribution of inflammation to fatigue before and during remission induction chemotherapy for AML and to study the predictive value of clinical factors, stress, and stool microbiome factors for fatigue.

Weekly fatigue and stress reports, blood, and stool samples were obtained from 105 patients with AML (max n per time point = 94) before (baseline) and during chemotherapy (week 2-4). Within every time point, fatigue was associated with stress (r 's=.33-.87) and with markers of inflammation (baseline: IL-6, TNF-alpha; week 2: IL-6, IL-7; week 3: IL-7, IL-15; week 4: IL-6, IL-15, VCAM-1; r 's=.33-.56. Stool microbiome diversity and abundance of specific microbiome strains were not associated with fatigue. Multiple regression models for inflammation predicting fatigue showed increased explained variances during chemotherapy: baseline, 21%; week 2-4, 29-49%. Adding stress to the models increased explained variances with 17% at baseline and 8% at week 2. In week 3 and 4, stress increased explained variances with 9% and 29%, respectively. These contributions of stress on fatigue were much lower than what would be expected from correlational analyses (31% and 76%). Exploratory mediation analyses showed stress to be a mediator of the relation between inflammation and fatigue in week 3 and 4.

In conclusion, stress and inflammation are independent predictors of fatigue before and in the early phases of chemotherapy, explaining almost 40% of variance in fatigue at these time points. Inflammation becomes a very strong driver of chemotherapy-related fatigue in week 3 and 4 of chemotherapy, possibly mediated by stress.

10. De novo discovery of candidate gene sets for the avian hair cell regeneration

Denise Duma and Andrew Groves Baylor College of Medicine, Houston, TX 77030

Loss of sensory hair cells is the major cause of hearing and balance disorders[3]. Sensory hair cells reside in sensory epithelia inside the ears of all vertebrates. Although mammals are unable to regenerate these epithelia once they have matured, some lower vertebrate species including birds are capable of sustained hair cell regeneration and thus reversal of hearing loss. As expected, the regeneration process is tremendously important and with large implications for medicine and human health, but unfortunately the underlying genetic mechanism is currently unknown. As a first step in unraveling this fascinating process, we seek to perform a clustering analysis of genes involved according to the major phenotypic events known to occur during regeneration following loss of hair cells. Secondly, a finer grained analysis of individual clusters should allow us to pinpoint hair cell specific markers. To this end, we perform gene expression analysis on two original datasets consisting of short time series of gene expression measurements in two relevant tissues, the chick utricle and cochlea. The datasets comprise each measurements of 17,685 genes across 7 time points 24 hours apart, roughly the time course necessary for regeneration following drug-induced damage of cultured hair cells. This is a difficult computational problem because we need to infer relationships between a large number of variables (genes) using a limited number of correlated measurements (timepoints). To reduce the dimensionality of our problem, we exploit the fact that we have both treated and control samples and at least two biological replicates for each tissue and perform a preliminary gene filtering, reducing the original gene set to around 3000 genes. We then use our filtered set of genes into a two-step clustering analysis, combining ideas from [1] with a spectral clustering step and automatic selection of the number of clusters. We manage to obtain clusters which are well separated and show significant enrichment in gene ontology (GO) terms relevant for the biological process at hand [2]. Further GO analysis of individual clusters allow us to identify a small number (around 30) of candidate hair cell marker genes.

11. Inhibition of mitochondrial p53 accumulation prevents cisplatin-induced neuropathy.

Magdalena Maj PhD¹, Ma Jiacheng PhD¹, Karen Krukowski PhD¹, Annemieke Kavelaars PhD¹, Cobi J. Heijnen PhD¹

¹Laboratory of Neuroimmunology, Department of Symptom Research, Division of Internal Medicine, The University of Texas MD Anderson Cancer Center, Houston, TX, USA

Chemotherapy-induced neurotoxicities like fatigue, cognitive impairment, and peripheral neuropathy are aversive side effect of cancer treatment. Currently, there are no drugs available that prevent these neurotoxicities. We studied the effects of the platinum-based anti-cancer drug cisplatin on the mitochondrial health status of peripheral nervous tissues and the occurrence of peripheral neuropathy. Moreover, we explored the effects of a mitochondrial protectant, pifithrin- μ (PFT- μ), on the development of cisplatin-induced peripheral neuropathy in relation to the mitochondrial function of peripheral nervous tissues of C57/Bl6 mice.

For the first time we show that cisplatin causes an aberrant bioenergetic profile (oxygen consumption rate, maximum respiratory capacity, ATP synthesis, and spare respiratory capacity) in dorsal root ganglion neurons and in peripheral nerve. Furthermore, cisplatin treatment results in ultrastructural morphological abnormalities in mitochondria of peripheral nervous tissues. On the molecular level we demonstrate that cisplatin induces a fast increase in mitochondrial p53 protein levels in dorsal root ganglia and sciatic nerves. Pre-treatment with a small molecule inhibitor of mitochondrial p53 accumulation, PFT- μ , prevented cisplatin-induced mitochondrial p53 accumulation, mitochondrial dysfunction and mitochondrial morphological abnormalities in peripheral nervous tissues. Remarkably, co-administration of PFT- μ also prevented chemotherapy-induced peripheral neuropathy as defined by mechanical allodynia and peripheral sensory loss.

Taken together, our results strongly suggest that an aberrant mitochondrial health status underlies cisplatin-induced neuropathy. Moreover, protecting mitochondrial function has the potential to become an efficacious therapeutic strategy for preventing chemotherapy-induced neurotoxicities in cancer patients.

12. Antineoplastic activity of CDK2/9 inhibitor CCT68127 occurs via induced anaphase catastrophe and inhibition of PEA15 phosphorylation in lung cancer

Masanori Kawakami¹, Lisa Maria Mustachio¹, Jaime Rodriguez-Canales², Barbara Mino², Jason Roszik^{3,4}, Lin Zheng¹, Pamela Andrea Villalobos², Carmen Behrens¹, Ignacio Wistuba², Xi Liu¹, Ethan Dmitrovsky^{1,5}

¹ Departments of ¹Thoracic/Head & Neck Medical Oncology, The University of Texas MD Anderson Cancer Center, Houston, TX

² Translational Molecular Pathology, The University of Texas MD Anderson Cancer Center, Houston, TX

³ Melanoma Medical Oncology, The University of Texas MD Anderson Cancer Center, Houston, TX

⁴ Genomic Medicine, The University of Texas MD Anderson Cancer Center, Houston, TX

⁵ Cancer Biology; The University of Texas MD Anderson Cancer Center, Houston, TX

We reported the first generation CDK2/9/7 inhibitor seliciclib (R-roscovitine, CYC202) exerts antineoplastic effects against lung cancer by inducing anaphase catastrophe. In anaphase catastrophe, cells with aneuploidy (a hallmark of cancer) cannot cluster supernumerary centrosomes, triggering abnormal anaphase and apoptosis. This study now finds the new CDK2/9 inhibitor CCT68127 (Cyclacel) is a more potent and selective CDK2 inhibitor than seliciclib. CCT68127 exerted substantial antineoplastic effects against diverse lung cancer cells. It inhibited growth, caused cell cycle arrest, and induced apoptosis more than did seliciclib. In a high throughput screen of 75 (57 *KRAS* wild-type and 18 *KRAS* mutant) lung cancer cell lines, those with *KRAS* mutation were significantly ($p < 0.05$) more sensitive to CCT68127 than *KRAS* wild-type cells. Anaphase catastrophe was triggered by CCT68127 treatment. Expression of 180 growth-regulatory proteins was studied after CCT68127 or vehicle treatments in murine (LKR13; *KRAS* mutant and ED1; *KRAS* wild-type) and human (Hop62; *KRAS* mutant and H522; *KRAS* wild-type) lung cancer cells using a reverse phase protein array (RPPA). The multifunctional growth regulator PEA15 (phosphoprotein enriched in astrocytes 15), exhibited Ser¹¹⁶ phosphorylation inhibition after CCT68127 treatment. This was independently confirmed by immunoblot analysis. When PEA15 was overexpressed, CCT68127 growth inhibition was antagonized, indicating its direct involvement in these effects. PEA15 knockdown using siRNAs repressed growth of lung cancer cells and enhanced growth inhibition after CCT68127 treatment. PEA15 immunohistochemical detection was explored in 235 human non-small lung cancers. PEA15 expression was reduced in lung cancers versus adjacent normal lung. Decreased PEA15 expression was associated with advanced stage and overall survival, establishing the translational importance of PEA15 expression in lung cancer. In summary, the novel CDK2/9 inhibitor, CCT68127, elicits marked antineoplastic effects in lung cancer. This occurs through mechanisms that engage anaphase catastrophe and reduce phosphorylation of the growth regulator PEA15.

13. Role of CDK9 inhibition as a sensitizer to radiation in esophageal adenocarcinoma: *in vitro* and *in vivo* efficacy study

Omkara Lakshmi Veeranki¹, Rashmi Dokey¹, Alicia Mejia¹, Zhimin Tong¹, Jianhu Zhang², Yuwei Qiao², Pankaj Kumar Singh², Riham Katkhuda³, Barbara Mino³, Jaime Rodriguez Canales³, Steven Lin⁴, Sunil Krishnan⁴ and Dipen Maru^{1,4}

¹Pathology, ²Experimental Radiation Oncology, ³Translational Molecular Pathology, ⁴Radiation Oncology, The University of Texas MD Anderson Cancer Center, Houston, TX

Preoperative chemoradiation in neoadjuvant setting is the standard of care for loco-regional esophageal adenocarcinoma (EAC). However, less than 30% of patients develop complete pathological response indicating need for newer therapeutic strategies. Cyclin dependent kinase 9 (CDK9) is found to be over expressed in EAC compared to Barrett's esophagus. Our previous studies demonstrated strong antitumor effects on inhibition of CDK9 in EAC both *in vitro* and *in vivo*. Here we report augmented tumor regression in irradiated xenografts on combination with Flavopiridol, a well-established clinically used CDK inhibitor, compared to single modality treatments. *In vitro* studies indicate that Flavopiridol could radiosensitize FLO-1 and SKGT4 EAC cells with sustained 53BP1 foci especially in SKGT4 cells. Flavopiridol and BAY1143572, a more selective inhibitor of CDK9, could radiosensitize additional EAC radiation sensitive and resistant cell lines (SKGT4-R, OE-33 and OE-33-R) as analyzed by MTT assay, apoptosis, formation of 53BP1 foci and clonogenic assay. Flavopiridol and BAY1143572 showed a radio-synergistic action by downregulating MCL-1 and Axl. In conclusion, the radio-sensitizing capacities of CDK9 inhibitors presented here suggest that their adjuvant administration might improve EAC therapy.

14. Dissecting the foreign body response to biomaterials by non-linear intravital microscopy

Eleonora Dondossola¹, Boris M. Holzapfel², Stephanie Alexander¹, Stefano Filippini¹, Dietmar W. Hutmacher², Peter Friedl^{1,3,4}

¹ David H. Koch Center for Applied Research of Genitourinary Cancers, The University of Texas MD Anderson Cancer Center, Houston, TX

² Institute of Health and Biomedical Innovation, Queensland University of Technology, Brisbane, Australia

³ Radboud University Medical Center, Nijmegen, The Netherlands

⁴ Cancer Genomics Centre, The Netherlands

Biomedical implants elicit and may fail due to a foreign body response (FBR) followed by fibrotic encapsulation of the material. Thus, dissecting the FBR mechanisms with innovative systems can drive interference approaches that display clinical relevance for patients. We here developed infrared-excited non-linear microscopy to resolve the 3D organization and fate of 3D printed scaffolds implanted into the deep mouse skin followed by a step-wise FBR. Immigrating myeloid cells, which engaged and became immobilized along the scaffold-tissue interface, converted to multinucleated giant cells as local producers of VEGF, which initiated and maintained an immature neovessel network followed by formation of a dense collagen capsule 2-4 weeks post-implantation. Consequently, elimination of the macrophage/giant cell compartment by clodronate and neutralization of VEGF by VEGF Trap, individually or in combination, strongly diminished giant cell accumulation, neovascularization and fibrosis. This identifies giant cells, via VEGF release and neovascularization, as main drivers of fibrotic encapsulation of engrafted material.

15. Limitations of The SHORT TEST OF FUNCTIONAL HEALTH LITERACY IN ADULTS (S-TOFHLA) as a Health Literacy Measure

Ashley J. Houston¹, Lisa M. Lowenstein¹, Diana Stewart Hoover², Viola B. Leal¹, Geetanjali R. Kamath¹, Robert J. Volk¹

¹ Department of Health Services Research, Division of Cancer Prevention & Population Sciences, The University of Texas MD Anderson Cancer Center, Houston, TX

² Department of Health Disparities Research, Division of Cancer Prevention & Population Sciences, The University of Texas MD Anderson Cancer Center, Houston, TX

Background: Despite the wide use of the Short Test of Functional Health Literacy in Adults (S-TOFHLA), misclassification of those with low health literacy have emerged.

Objective: Explore the limitations of the S-TOFHLA in identifying people with low health literacy compared to validated measures of health literacy.

Design: Secondary data analysis of a randomized controlled trial.

Settings: Large, urban academic medical center and a community-based organization.

Participants: English-speaking, aged 45-75 years, without increased risk for colorectal cancer.

Measurements: Participants completed the S-TOFHLA and three additional measures of health literacy: the Brief Health Literacy Screen (BHLS), the Subjective Numeracy Scale (SNS), and the Graphical Literacy Assessment. For scoring, we used the established categories based on existing cut-points or the median split.

Results: Participant (n=187) median age was 58 years (range 45-75 years). Most (70%) identified as being Black or African American, 63% (n=118) were women, and 53% reported completing some college or a college degree. Of those who scored “adequate” on the S-TOFHLA, 86% (n=113) scored low on at least one total or subscale score and 63% (n=82) scored low on at least one total score. For the other health literacy assessments, of those who scored “adequate” on the S-TOFHLA, 15% (n=20) scored low on the BHLS, 50% (n=67) scored low on the SNS, and 40% (n=39) scored low on Graphical Literacy.

Limitations: The broad use of the S-TOFHLA may contribute to miscategorizing people into adequate health literacy, as evidenced by the low scores on the other health literacy assessments.

Conclusion: The S-TOFHLA is the most widely used measure of health literacy; however, the current findings suggest that it underestimates individuals’ health literacy. Efforts are needed to develop more encompassing tools for use in research and clinical practice.

16. Affective Modulation of the Late Positive Potential Following Repeated Exposure to Cigarette Cues in Smokers and Never-smokers

Menton M. Deweese¹, Hannah L. Stewart¹, Kimberly N. Claiborne², Jennifer Ng¹, Paul M. Cinciripini¹ and Francesco Versace³

¹Department of Behavioral Science, The University of Texas MD Anderson Cancer Center, Houston, TX.

²Department of Psychology, Rice University, Houston, TX.

³Department of Family and Preventive Medicine, The University of Oklahoma Health Science Center, Oklahoma City, OK.

In the laboratory, smokers reliably demonstrate higher reactivity to cues that have previously been associated with their addiction to nicotine; however, recent studies have reported that never-smokers also show enhanced brain responses to cigarette-related stimuli, albeit less than smokers. Here, we recorded event-related potentials (ERPs) derived from the electroencephalogram (EEG) using a repetitive picture-viewing paradigm to assess the effects of stimulus repetition on the amplitude of the late positive potential (LPP) in a sample of 38 smokers and 37 never-smokers. We predicted that the LPP amplitude elicited by pleasant and unpleasant stimuli would remain significantly greater than neutral for both smokers and never-smokers, but that only smokers would maintain the significant difference in LPP amplitude to cigarette-related cues compared to neutral following stimulus repetition. Enhanced LPP amplitude to cigarette cues in smokers, and a habituation the LPP response to cigarette cues in never-smokers would demonstrate that cigarette cues are motivationally relevant stimuli only for smokers. In line with our hypothesis, we observed greater LPP amplitude to pleasant and unpleasant cues relative to neutral, in both smokers and never-smokers, averaged across repetition blocks. Also in line with our hypothesis, we observed a consistently greater LPP response to cigarette cues relative to neutral in smokers, following stimulus repetition. Never-smokers did not show this effect. While smokers and never-smokers reported no difference in self-reported stimulus ratings of pleasant, unpleasant, or neutral stimuli, the never-smokers rated smoking cues as unpleasant. In sum, cigarette cues are perceived as unpleasant for never-smokers, whereas for smokers these cues have acquired significance through repeated pairing with nicotine.

17. A mouse model of neurodegeneration

Li Lu (6th APSS)

Neurodegenerative diseases are characterized as progressive neuron damage/death and brain functional deterioration. Common symptoms are ataxias and dementias, which severely impacts patients' and their caregivers' life style. Although researchers have been able to characterize different neurodegenerative diseases such as Alzheimers's disease (AD), Parkinson's disease (PD), and Huntington's disease (HD) according to the symptoms, their causes and the biological mechanisms are still largely unknown. Here we described a mouse model that shows fast neurodegeneration and severe brain functional deterioration. The model offers an *in vivo* system to study the molecular mechanism of neurodegenerative disease, and may help develop potential treatments for some, if not all neurodegenerative diseases.

18. 3-D TRACT-SPECIFIC FUNCTIONAL ANALYSIS OF WHITE MATTER INTEGRITY IN ALZHEIMER'S DISEASE

Yan Jin¹, Chao Huang¹, Hongtu Zhu¹

¹ Department of Biostatistics University of Texas MD Anderson Cancer Center Houston, Texas, USA

Diffusion-weighted MRI (DWI) is increasingly used to examine white matter (WM) integrity, revealing microstructural abnormalities not detectable with traditional structural MRI. In studies of Alzheimer's disease (AD), traditional methods are not able to demonstrate the alterations of WM tracts in 3-D. Here we propose a complete 3-D tract-based analysis (TSA) framework to study WM degeneration in AD in a cohort of 200 subjects. It combines our recently developed methods, known as autoMATE (automated Multi-Atlas Tract Extraction) [1] and FADTTS (Functional Analysis for Diffusion Tensor Tract Statistics) [2].

Material and Methods

Our 200 subjects (49 normal controls - NC, 111 Mild Cognitive Impairments - MCIs, and 40 ADs) were from the ADNI database [3]. DWI images were acquired with 46 image volumes per subject with 2.7 mm isotropic resolution ($b=1,000$ s/mm²). The whole-brain probabilistic tractography was performed with Camino [4]. We employed autoMATE to anatomically extract and cluster WM tracts from the tractography. The 18 major extracted WM tracts were: left (L)/right (R) anterior thalamic radiation (ATR), L/R cingulum (CNG), L/R corticospinal tract (CST), L/R inferior fronto-occipital fasciculus (IFO), L/R inferior longitudinal fasciculus (ILF), fornix (FNX), L arcuate fasciculus (ARC), and six segments of the corpus callosum (CC) projecting to the frontal lobes (CC-FRN), precentral gyri (CC-PRC), postcentral gyri (CC-POC), superior parietal lobes (CC-PAR), temporal lobes (CC-TEM), and occipital lobes (CC-OCC). Finally, we performed statistical analysis on the 3-D fractional anisotropy (FA)/mean diffusivity (MD) profiles of those 18 WM tracts with FADTTS [2], a functional analysis method that models how diffusion parameters along the WM fiber tract associate with a set of covariates, such as diagnostic status.

Results

Fig. 1 illustrates the tract labeling results. WM alterations are noted in the gradually decreasing numbers of fibers from NC to MCI to AD, in the genu of CC. **Figs. 2** and **3** illustrate the 3-D FA and MD profiles of the 18 WM tracts in the pairwise group comparisons, respectively. Group differences were considered statistically significant at points with $-\log$ values > 1.3 ($p=0.05$).

Conclusion

Here we presented an overall framework to conduct TSA of WM in AD. Unlike prior studies, our TSA shows detailed 3-D profiles of group differences in diffusion parameters, on individualized 3D models of tracts.

Fig.1. Representative clustering results for 18 WM tracts in individuals from the three groups (NC, MCI, and AD). *Left side, back, and top* views of tract overlays are displayed.

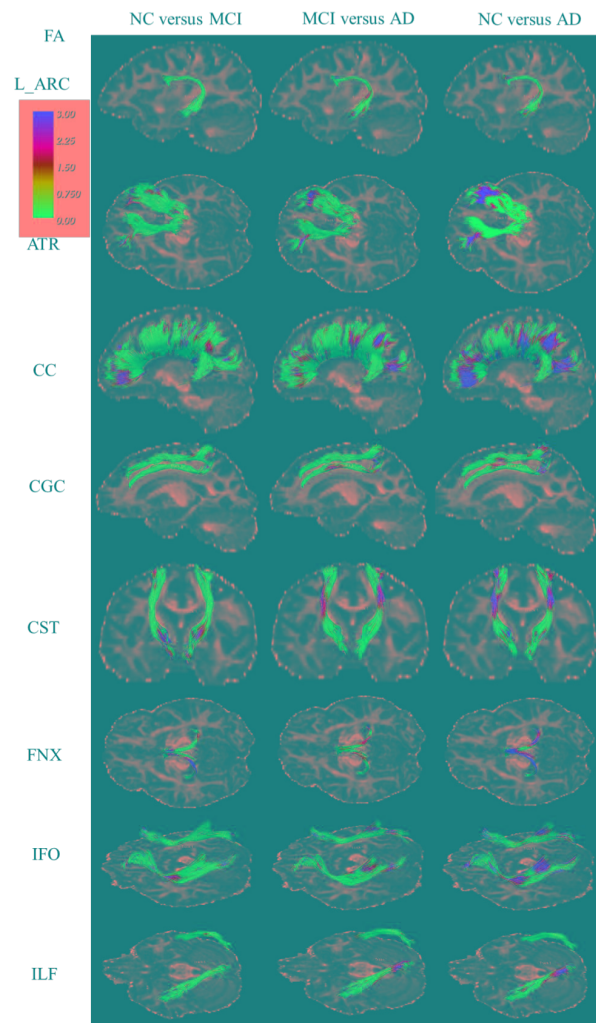
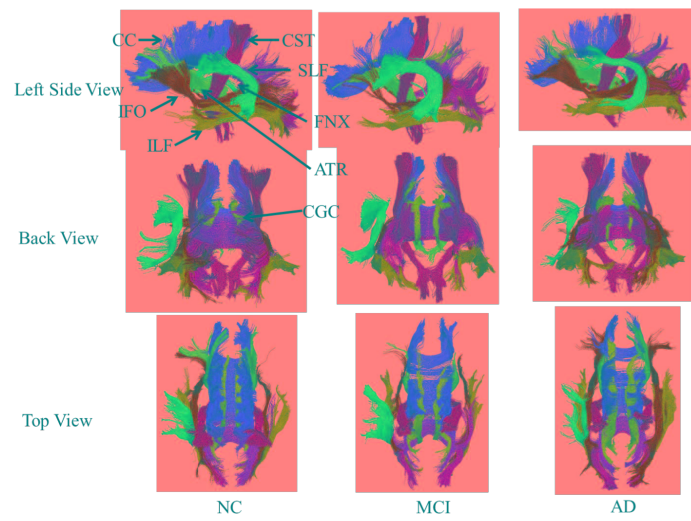


Fig. 2. 3-D FDR corrected color maps of the 18 WM tracts reveal differences in FA values in comparisons of the three diagnostic groups.

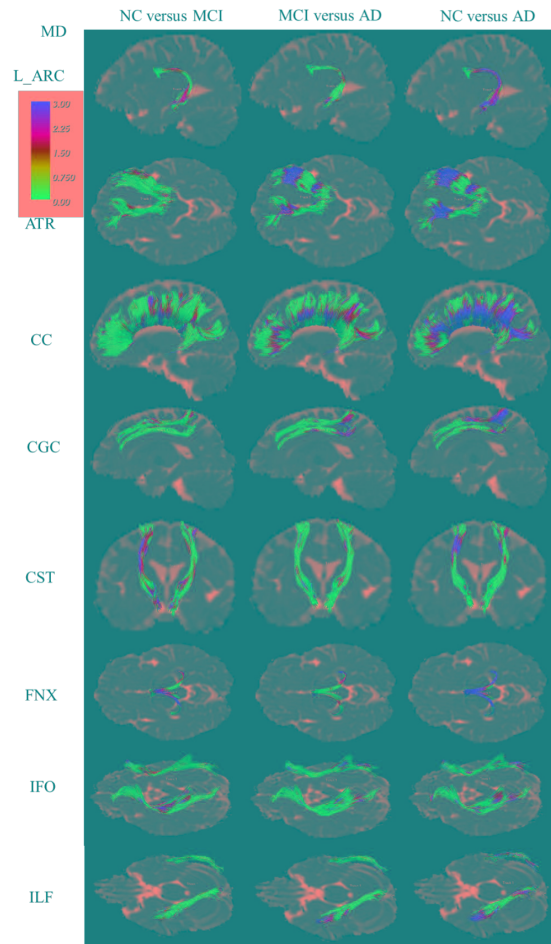


Fig. 3. 3-D FDR corrected color maps of the 18 WM tracts reveal differences in MD values in comparisons of the three diagnostic groups.

19. A Cell-autonomous Mammalian 12-hour Clock Coordinates Metabolic and Stress Rhythms

Bokai Zhu¹, Qiang Zhang², Clifford C. Dasco^{1,2,3}, Athanasios C. Antoulas^{2, ¶} and Bert W. O'Malley^{1,4, ¶, ††}

¹ Department of Molecular and Cellular Biology, Baylor College of Medicine, Houston, TX

² Department of Electric and Computer Engineering, Rice University, Houston, TX

³ Department of Medicine, Baylor College of Medicine, Houston, TX

⁴ Dan L. Duncan Cancer Center, Baylor College of Medicine, Houston, TX

¶ These authors contributed equally to this work.

Besides circadian rhythms, oscillations cycling with 12h period also exist. However, the prevalence, origin, regulation and function of the mammalian 12h rhythms remain elusive. Utilizing a novel non-parametric mathematical approach that unbiasedly identifies all superimposed oscillations, we uncovered wide-prevalence of 12h gene expression and metabolism rhythms in mouse liver, which is coupled with physiological 12h UPR oscillation. Importantly, the mammalian 12h rhythm is cell-autonomous, driven by a dedicated 12h pacemaker distinct from the circadian clock, can be established *in vitro* by metabolic and ER stress cues, and functions to coordinate stress and metabolic fluctuations to ensure systematic homeostasis. Mechanistically, we identified UPR transcription factor XBP1s as a transcriptional regulator of mammalian 12h clock. We further postulated that the mammalian 12h clock is evolved from the circatidal clock of marine animals. The discovery of a cell-autonomous mammalian 12h clock will shed new lights on how perturbed biological rhythms cause human diseases.

20. A novel method for imaging the pharmacological effects of antibiotic treatment on *Clostridium Difficile*

Endres BT^{*1}, Bassères E¹, Memariani A³, Chang L², Alam MJ¹, Kakadiaris IA³, Chesnel L⁴, Garey KW¹

¹ Department of Pharmacy Practice and Translational Research, ²Department of Electrical and Computer Engineering, ³Department of Computer Science University of Houston, Houston, Texas, USA;

⁴Merck and Co., Inc. Kenilworth, New Jersey, USA

Clostridium difficile is a gram-positive anaerobic bacteria that is a significant cause of hospital-acquired diarrhea that can lead to mortality. Current treatment options for *C. difficile* infection (CDI) are limited, however, new antibiotics are currently being developed that will require rigorous assessment of efficacy. Current methods for determining antibiotic effectiveness on *C. difficile* are over-simplistic and do not shed light on the drug's mechanism of action (MOA). Because of this, we developed a novel protocol utilizing both scanning electron microscopy (SEM) with drug killing curves to determine the efficacy and visualize the phenotypic response to drug treatment. To test the value of this approach, supraMIC kill curves were conducted using vancomycin, metronidazole, and fidaxomicin, all of which are currently used to treat CDI and have defined, yet different MOA's. Following collection, cells were either plated or imaged using an SEM. Consistent with previous reports, we found that both vancomycin, metronidazole, and fidaxomicin had significant bactericidal activity following 24h of treatment ($>4 \log_{10}$ difference; $P<0.05$). By SEM imaging the cells and developing a semi-automatic pipeline for analyzing the images, we were able to determine that vancomycin significantly affected the cell wall ($+\Delta 116\%$ in cell wall deformation; $P<0.05$) compared to other antibiotic treatments and control cells. In contrast, fidaxomicin and metronidazole had significant effects on cell length ($>50\%$ reduction for each; $P<0.05$) compared to controls and vancomycin-treated cells. While the phenotypic response to drug treatment has not been documented previously in this manner, they are consistent with the drug's MOA demonstrating the versatility and reliability of the imaging and measurements and the application of this technique for other experimental compounds.

21. Targeting immunotherapy to metastatic cancers enhancing oncolytic viruses with immune checkpoints modulation

Francisco W. Puerta Martinez¹

¹ The University of Texas MD Anderson Cancer Center

Metastasis of advanced stage cancers remains as the main cause of morbidity and mortality in oncologic patients. Metastatic cancers, especially those that metastasize to the brain, are generally resistant to conventional therapies. Thus, more innovative and efficacious therapies are urgently needed. Therapeutic goals are the specific targeting of malignant cells, shrinkage of established tumors, prevention and/or eradication of metastases and, ultimately, induction of a specific anti-tumor immune response. In this study we tested the efficiency of a treatment regimen consisting of oncolytic adenoviruses combined with specific immune checkpoints regulators to prevent tumor progression and metastasis. To do so, the mouse metastatic breast cancer cells 4T1, were orthotopically implanted in female BALB/c mice. The resulting primary tumors were treated with up to 10 doses of third generation adenoviruses targeting different immune checkpoints, such as, OX40/OX40L and GITR/GITRL pathways in the immune synapse. The treatment with these adenoviral constructs resulted in T cells activation and reduction of the metastases in 50% of the mice. In addition the size and number of the metastases were significantly lower comparing with those observed in the control groups. We are also testing these newly developed armed oncolytic viruses as single treatment and in combination with immune checkpoint antibodies, such as, PD-1 to ascertain the optimum combination that potentially could be translated to a clinical trial.

22. mTORcise: Replicating Exercise Induced Remodeling of the Heart by targeted deletion of Tuberin.

Giovanni Davogustto¹, Rebecca Salazar¹, Hernan Vasquez¹, Patrick Guthrie, Heinrich Taegtmeyer,

¹University of Texas Health Science Center at Houston, Houston, TX

Introduction: When stressed, the heart remodels metabolically and structurally. Metabolically, the heart increases its reliance on carbohydrates for energy provision, while structurally, it hypertrophies. Whether both processes occur independently, or if they are interrelated is not known. In the heart, the activation of the mechanistic Target Of Rapamycin Complex 1 (mTORC1) pathway is closely tied to glucose metabolism and cellular growth, and is therefore a potential link between these two types of remodeling.

Objective: We examined whether long-term, sustained mTORC1 activation results in metabolic and structural remodeling in the heart, with a focus on the time course of these events.

Methods: We developed a mouse model of inducible, cardiac-specific deficiency of tuberin (TSC2), a key inhibitor of mTORC1. TSC2 gene recombination was induced between 5-7 weeks of age, and echocardiograms were performed at 4, 10 and 20 weeks after induction. Genomic DNA, total RNA and proteins were extracted from freeze-clamped hearts for PCR, real-time PCR and immunoblotting respectively. Glucose 6-phosphate (G6P) levels were measured by spectrophotometric enzymatic analysis. Histologic analysis using H/E and Masson's Trichrome stains were used to determine cardiomyocyte area and interstitial fibrosis.

Results: Immunoblotting of protein markers confirmed TSC2 knockout (KO) and activation of mTORC1 downstream targets as early as two weeks after induction. G6P was increased 4 weeks after induction, before any structural changes were detected. Serial echocardiograms revealed concentric remodeling 10 weeks after induction, which persisted at 20 weeks. Furthermore, the systolic function in the conditional KO animals was greater than the controls 20 weeks after induction. Cardiomyocytes hypertrophied at 20 weeks, without any evidence of increase in fibrosis.

Conclusions: Inducible, sustained mTORC1 activation by TSC2 KO in the heart triggers physiologic remodeling, characterized by cardiomyocyte hypertrophy, concentric remodeling and improved systolic function. This phenotype is similar to the one induced by strength training. Lastly, we show that metabolic remodeling precedes this type of structural remodeling.

23. *In vitro* Demonstration of the Channel Activity of an Anion Channelrhodopsin

Hai Li¹, Oleg A. Sineshchekov¹, Gang Wu^{1,2}, John L. Spudich¹

¹Center for Membrane Biology, Department of Biochemistry and Molecular Biology, University of Texas Health Science Center at Houston McGovern Medical School, Houston, TX 77030

²Department of Internal Medicine, University of Texas Health Science Center at Houston McGovern Medical School, Houston, Texas 77030

Light-gated cation-conducting channelrhodopsins (CCRs), phototaxis receptors that depolarize the plasma membrane in algae, have been widely used to photoactivate neuron firing in brain research, enabling neural circuitry mapping of brain functions, animal studies of neurological diseases, and recently have begun to be used in human clinical trials as gene therapy agents to restore vision to blind individuals. Clinical optogenetics necessarily began with a neuron-activating CCR because efficient neuron inhibitors were not available. The recently discovered anion-conducting channelrhodopsins (ACRs, Govorunova et al. 2015 Science 349:647-650), in addition to their interest as a previously unknown phenomenon in nature, have generated much interest as optogenetic tools because of their unprecedented photoefficiency to silence neurons by light-gated chloride conduction. ACRs open the way for gene therapy for conditions in which excessive neural firing needs to be suppressed. Neuron hyperactivity is centrally involved either as a cause or as a major symptom in myriad neural pathologies. Elucidation of the mechanisms of ACR conductance and of their kinetic and spectral properties will facilitate optimization of ACRs for clinical therapies. For such studies we have developed a functional *in vitro* system with reconstituted detergent-purified ACR incorporated into large unilamellar vesicles (LUVs). Light-induced Cl⁻ currents through the ACRs are monitored by a passive flux of protons sensed by the pH-sensitive fluorescent dye pyranine in the LUV lumen. EPR assessment of spin-label accessibility shows that the ACR proteins insert uniformly inside-out, i.e the cytoplasmic side of the protein faces the extravesicular medium. This system provides the first *in vitro* measurement of channelrhodopsin conductance in a system amenable to measurement of both function (ion currents) and structural changes by optical and molecular spectroscopy. Initial measurements with the LUVs confirm our *in vivo* findings (Sineshchekov et al. 2016 PNAS 113:E1993-2000) indicating that channel opening occurs prior to proton transfer from the retinylidene chromophore to the protein. Channel closing involves the deprotonation of the chromophore in ACRs in stark contrast to CCRs in which channel opening is preceded by proton release from the chromophore. Further progress will be discussed.

24. A Novel Schema to Enhance Data Quality of Patient Safety Event Reports

Hong Kang¹, Yang Gong¹.

School of Biomedical Informatics, the University of Texas Health Science Center at Houston, Houston, TX, USA

The most important knowledge in the field of patient safety is regarding the prevention and reduction of patient safety events (PSEs). It is believed that PSE reporting systems could be a good resource to share and to learn from previous cases. However, the success of such systems in healthcare is yet to be seen. One reason is that the qualities of most PSE reports are unsatisfactory due to the lack of knowledge output from reporting systems which makes reporters report halfheartedly. In this study, we designed a PSE similarity searching model based on semantic similarity measures, and proposed a novel schema of PSE reporting system which can effectively learn from previous experiences and timely inform the subsequent actions. This system will not only help promote the report qualities but also serve as a knowledge base and education tool to guide healthcare providers in terms of preventing the recurrence and serious consequences of PSEs.

25. HDAC6 Inhibition Effectively reverses Chemotherapy-Induced Peripheral Neuropathy.

Jiacheng Ma¹, Karen Krukowski¹, Olga Golonzhka², Tanuja Gutti¹, Matthew Jarpe², Cobi J. Heijnen¹, Annemieke Kavelaars¹

¹ The University of Texas MD Anderson Cancer Center. 2. Acetylon Pharmaceuticals.

Chemotherapy-induced peripheral neuropathy (CIPN) characterized by pain and numbness is one of the most commonly reported side-effects of cancer treatment. The presence of CIPN can limit the dosage and interfere with the selection of chemotherapeutics, delay further treatment cycles, or in the worst scenario lead to early termination of treatment. Despite daunting facts about the high prevalence and severity of CIPN, there is less known about its underlying mechanism or effective treatment. HDAC6, a microtubule-associated deacetylase, plays an important role in the regulation of α -tubulin-dependent intracellular transport. Inhibition of HDAC6 has been shown protective in several neurological disorders through enhancing α -tubulin acetylation, and thereby improving axonal transport of mitochondria. In the current study, we aim at investigating that if inhibition of HDAC6 could prevent and/or reverse cisplatin-induced peripheral neuropathy. We show that pharmacological inhibition of HDAC6 with the selective HDAC6 inhibitor ACY-1083 both prevented and reversed cisplatin-induced mechanical allodynia. In addition, ACY-1083 reversed established spontaneous pain as well as numbness induced by cisplatin. Mechanistically, ACY-1083 treatment increased α -tubulin acetylation in neuronal tissues. More importantly, ACY-1083 restored the impaired mitochondrial motility induced by cisplatin in primary cultures of DRG neurons in vitro, and restored mitochondrial function and content in the distal tibial nerves in vivo. ACY-1083 also restored intra-epidermal nerve fiber (IENF) density in cisplatin-treated mice. Our results strongly indicate that HDAC6 inhibition protects against cisplatin-induced peripheral neuropathy, and the protective effects are likely exerted through enhancing mitochondrial transport and improving mitochondrial bioenergetics in the distal sensory axons.

26. PEA-15 (phosphoprotein enriched in astrocytes) regulates epithelial-mesenchymal transition and invasive behavior through its phosphorylation in triple negative breast cancer

Jihyun Park¹, Evan N. Cohen², Jangsoon Lee¹, Naoto T. Ueno¹, Debu Tripathy¹, James M. Reuben², Chandra Bartholomeusz¹

¹ Section of Translational Breast Cancer Research, Department of Breast Medical Oncology, The University of Texas MD Anderson Cancer Center, Houston, Texas, USA

² Department of Hematopathology, The University of Texas MD Anderson Cancer Center, Houston, Texas, USA

Triple-negative breast cancer (TNBC) is an aggressive subtype with no proven active targeted therapies available. Patients with TNBC have a very poor prognosis because the disease often metastasizes. Newer approaches to preventing metastasis and inhibiting tumor growth, are crucial to improving prognosis for these patients. Previously it has been shown that PEA-15 binds to ERK, preventing ERK from being translocated to the nucleus and hence blocking its activity. Our previous studies showed that overexpression of wild type PEA-15 inhibited ERK activity and reduced tumor volume in a TNBC xenograft model. We also showed that PEA-15 being unphosphorylated at both Ser104 and Ser116 inhibited ovarian cancer cell tumorigenicity. However, the function and impact of PEA-15 phosphorylation on TNBC is not well understood. From these observations, we hypothesized that unphosphorylated PEA-15 will prevent metastasis in TNBC through the inhibition of EMT.

To study the effect of the phosphorylation status of PEA-15 on metastasis in TNBC, we established stable cell lines overexpressing nonphosphorylatable (PEA-15-AA) and phosphomimetic (PEA-15-DD) mutants in MDA-MB-468 cells. The clonogenic growth of PEA-15-AA was significantly reduced by 80% compared with vector control, PEA-15-V. Anchorage-independent growth, an indicator of *in vivo* tumorigenicity, of PEA-15-AA was inhibited by 60% compared with PEA-15-V. PEA-15-AA upregulated the expression of E-cadherin, a key epithelial molecular marker and decreased expression of vimentin, a mesenchymal marker suggesting that PEA-15-AA reverses EMT. Next, we investigated whether PEA-15-AA had inhibited migration and invasion of TNBC cells. Compared with PEA-15-V, migration and invasion of PEA-15-AA were reduced by 65% and 72%, respectively. To determine the mechanism of how PEA-15 regulates EMT and metastasis we performed RT-PCR immune and metastasis arrays. We found that the cytokine expression levels of IL-8 and PDGF-BB were greatly decreased in PEA-15-AA. Upon stimulation of the PEA-15-AA with those cytokines, mesenchymal characteristics were partially rescued indicating that PEA-15-AA may inhibit these cytokines, thereby reversing EMT. Next, NOD/SCID mice were injected with MDA-MB-468 stable cells into the mammary fat pad. The PEA-15-DD-injected group showed an increase in tumor volume compared with PEA-15-V and PEA-15-AA groups, suggesting that PEA-15-AA has antitumor effects both *in vitro* and *in vivo*. Further studies are warranted to determine the correlation between the phosphorylation status of PEA-15 and expression of cytokines in regulating metastasis in TNBC. Together, this study highlights the potential for overexpression of unphosphorylated PEA-15 as an approach for TNBC-targeted therapy.

27. HPRM: Hierarchical Principal Regression Model of Diffusion Tensor Bundle Statistics

Jingwen Zhang¹, Joseph G. Ibrahim¹, Hongtu Zhu^{1,2}

¹ Department of Biostatistics, The University of Texas MD Anderson Cancer Center, Houston, TX

² Biomedical Research Imaging Center, University of North Carolina at Chapel Hill, NC

In a typical diffusion tensor Imaging (DTI) study, diffusion properties are observed among multiple fiber bundles to understand the association between neurodevelopment and clinical variables, such as age, gender, biomarkers, etc. Most research focuses on individual tracts or use summary statistics to jointly study a group of tracts, which usually ignores the global and individual functional structures. To address this problem, we propose a hierarchical functional principal regression model, consisting of three components: (i) a multidimensional Gaussian process model to characterize functional data, (ii) a latent factor model to jointly analyze multiple fiber bundles and to capture common effect shared among tracts, and (iii) a multivariate regression model study tract-specific effect. A multilevel estimation procedure is proposed and a global statistic is introduced to test hypothesis of interest. Simulation is conducted to evaluate the performance of HPRM in estimating shared effect and individual effect. We also applied HPRM to a genome-wide association study (Gwas) of one-year twins to explore important genetic markers in brain development among young children.

28. Levetiracetam mitigates doxorubicin-induced DNA and synaptic damage in neurons

Jose Felix Moruno Manchon¹, Yuri Dabaghian^{2,3}, Nnidi-Ese Uzo^{1,5}, Shelli R. Kesler⁴, Jeffrey S. Wefel⁴, and Andrey S. Tsvetkov^{1,5}

¹Department of Neurobiology and Anatomy, University of Texas, Houston Medical School, Houston, TX

²The Jan and Dan Duncan Neurological Research Institute, Baylor College of Medicine, Houston, TX

³Department of Computational and Applied Mathematics, Rice University, Houston, TX

⁴Department of Neuro-Oncology, M.D. Anderson Cancer Center, Houston, TX

⁵The University of Texas Graduate School of Biomedical Sciences, Houston, TX

Neurotoxicity may occur in cancer patients and survivors during or after chemotherapy. Cognitive deficits associated with neurotoxicity can be subtle or disabling and frequently include disturbances in memory, attention, executive function and processing speed. Searching for pathways altered by anti-cancer treatments in cultured primary neurons, we discovered that doxorubicin, a commonly used anti-neoplastic drug, significantly decreased neuronal survival. The drug promoted the formation of DNA double-strand breaks in primary neurons and reduced synaptic and neurite density. Pretreatment of neurons with levetiracetam, an FDA-approved anti-epileptic drug, enhanced survival of chemotherapy drug-treated neurons, reduced doxorubicin-induced formation of DNA double-strand breaks, and mitigated synaptic and neurite loss. Thus, levetiracetam might be part of a valuable new approach for mitigating synaptic damage and, perhaps, for treating cognitive disturbances in cancer patients and survivors.

29. Regulation of exosome secretion in ovarian cancer

Justyna Filant¹, Pinar Kanlikilicer², Mohammed H. Rashed², Andreia Silva ², Cristina Ivan², Cristian Rodriguez-Aguayo², Theresa J. O'Halloran³, George A. Calin², Gabriel Lopez-Berestein², Anil K. Sood¹

¹Department of Gynecologic Oncology & Reproductive Medicine; ²Department of Experimental Therapeutics, UT MD Anderson Cancer Center; ³Department of Molecular Biosciences, UT at Austin

Evidence indicates that the release of microRNAs (miRs) from cells into extracellular fluid is a selective process that correlates with various diseases, including cancer. Cancer cells can modulate the gene expression of cells in the tumor microenvironment or in distant pre-metastatic sites via secreted miRs. However, the mechanisms regulating miR release and the specific role of secreted miRs in cancer initiation and progression remain unclear. To identify candidate molecules that regulate miR secretion, we performed a functional small interfering RNA (siRNA) screen in ovarian cancer cells and found that cyclin-dependent kinase 5 (CDK5) emerged as the top molecule. CDK5 knockdown altered multivesicular body (MVB) fusion with the cell plasma membrane, reduced exosome release, and thereby impaired miR secretion. Silencing CDK5 *in vivo* using a neutral nanoliposomal delivery system resulted in robust reduction of tumor burden in orthotopic mouse models of ovarian cancer. Ectopic expression of CDK5 stimulated tumor growth in a mouse model of ovarian cancer, whereas blockade of exosome biogenesis reversed this effect. Thus, CDK5 inhibition provides a novel and robust strategy for reducing exosomal miR secretion in cancer.

30. Nuclear proteolysis in the regulation of metabolic genes in multiple myeloma

Laure Maneix^{1,2,3}, Fu-Yuan Shih^{1,2,3}, Polina Iakova^{1,2,3}, Joanne Ino Hsu^{1,2,3}, Andre Catic^{1,2,3,4}

¹ *Huffington Center on Aging, Baylor College of Medicine, Houston, TX*

² *Dan L. Duncan Comprehensive Cancer Center, Baylor College of Medicine, Houston, TX*

³ *Stem Cells and Regenerative Medicine Center (STaR Center), Baylor College of Medicine, Houston, TX*

⁴ *Department of Molecular and Cellular Biology, Baylor College of Medicine, Houston, TX*

The dynamic interaction of transcription factors (TFs) with promoters and enhancers allows cells to continuously adjust gene expression. Whereas the composition and binding of TFs at genomic sites is the focus of a widespread research effort, relatively little is known about how these complexes are being removed. We previously devised a method to detect genomic locations that are associated with nuclear protein turnover mediated by the ubiquitin-proteasome system (UPS).

Multiple myeloma, the second most common hematopoietic malignancy, has become a model disease for drugs that interfere with the UPS through either blocking or facilitating protein elimination. The proteasome inhibitor Velcade, for instance, has become first-line treatment in myeloma. Yet, our knowledge of how myeloma cells are killed by this drug is incomplete. Our research is focused on defining how proteolysis regulates transcriptional dynamics in this disease and how this impacts Velcade sensitivity.

Following proteasome inhibition, we are utilizing next generation sequencing to identify sites of nuclear protein turnover and evaluate epigenetic changes. Our aim is to identify TFs that may qualify as more specific targets for treatment compared to blunt proteasome inhibition. Our findings reveal that certain TFs, including metabolic and cell growth regulators, are particularly sensitive to Velcade. Among these transcriptional regulators, the co-repressor NCoR1 plays a key role in controlling cell metabolism by adjusting mitochondrial gene expression. We are currently validating the mechanism of NCoR1 degradation, with a particular emphasis on the new role of its E3-ubiquitin ligase Seven in absentia 2 (Siah2) in mitochondrial regulation, to better understand how this degradation pathway impacts myeloma proliferation and metabolism.

This research project will contribute to our understanding of epigenetic and transcriptional dynamics in multiple myeloma. With the focus on gene programs that are continuously adapting or changing, we seek to unlock new targets for molecular therapy. More particularly, our observations suggest that the Siah2/NCoR1 axis may be an attractive target for the treatment of multiple myeloma.

31. Loss of the ISG15 protease USP18 mislocalizes and destabilizes KRAS in lung cancer

Lisa Maria Mustachio¹, Jaime Rodriguez-Canales², Ignacio Wistuba², Hiroyuki Katayama³, Samir Hanash³, Jason Roszik^{4,5}, Masanori Kawakami⁶, Xi Liu⁶, and Ethan Dmitrovsky^{1,6,7}

¹Departments of Pharmacology and Toxicology, Geisel School of Medicine, Hanover, NH; Departments of ²Translational Molecular Pathology, ³Clinical Cancer Prevention, ⁴Melanoma Medical Oncology, ⁵Genomic Medicine, ⁶Thoracic/Head and Neck Medical Oncology, and ⁷Cancer Biology, The University of Texas MD Anderson Cancer Center, Houston, TX.

KRAS is frequently mutated in lung cancers. Innovative strategies are needed to combat *KRAS* mutant lung cancers because these tumors are often resistant to therapy. This study extends our previous work by reporting that loss of USP18 can destabilize the *KRAS* oncoprotein in murine and human lung cancer cells. In contrast, engineered gain of USP18 expression introduced into the same panel of lung cancer cells stabilized *KRAS* protein. Loss of USP18 expression in *KRAS* mutant-expressing lung cancer cells inhibited their growth while gain of USP18 expression opposed this effect. Intriguingly, immunoprecipitation assays established that *KRAS* conjugates with the ubiquitin-like protein ISG15. This leads to *KRAS* protein destabilization. To independently confirm that *KRAS* directly complexes with ISG15, site-directed mutagenesis was performed to render the C-terminal domain of *KRAS* lysine-less. This led to stabilization of *KRAS*, despite knockdown of USP18. These studies were confirmed and extended in the *in vivo* setting of *KRAS*-driven lung cancers in *KRAS*^{LA2/+} mice. We crossed these mice with *USP18*^{-/-} null mice to obtain *KRAS*^{LA2/+}*USP18*^{-/-} compound mice. Strikingly, these compound mice had statistically significantly reduced lung cancers as compared to parental *KRAS*^{LA2/+} mice. USP18 immunohistochemical expression was compared in these engineered mice versus a second engineered mouse lung cancer model driven by aberrant cyclin E expression. USP18 expression was substantially higher in the *KRAS*-driven than cyclin E-dependent murine lung cancers. To explore the translational relevance of this work, lung cancer tissue arrays were examined in lung tumors. USP18 expression was significantly higher in *KRAS* mutant adenocarcinomas as compared to wild-type cases. Taken together, these studies broaden the role of USP18 as an antineoplastic target to combat lung cancers that harbor *KRAS* mutations.

32. TBD

33.ZMYND8 reads the dual histone mark H3K4me1-H3K14ac to antagonize the expression of metastasis-linked genes

Na Li^{1,14}, Yuanyuan Li^{2,3,14}, Jie Lv^{4,5,6,14}, Xiangdong Zheng^{2,3}, Hong Wen⁷, Hongjie Shen⁸, Guangjing Zhu⁹, Tsai-Yu Chen¹, Shilpa S. Dhar¹, Pu-Yeh Kan¹, Zhibin Wang⁹, Ramin Shiekhataar¹⁰, Xiaobing Shi⁷, Fei Lan⁸, Kaifu Chen^{4,5,6}, Wei Li^{11,*}, Haitao Li^{2,3,12,*}, and Min Gyu Lee^{1,13,*}

¹Department of Molecular and Cellular Oncology, The University of Texas MD Anderson Cancer Center, 1515 Holcombe Blvd., Houston, TX 77030, USA

Histone acetylation, including acetylated H3K14 (H3K14ac), is generally linked to gene activation. Monomethylated histone H3 lysine 4 (H3K4me1), together with other gene-activating marks, denotes active genes. In contrast to usual gene-activating functions of H3K14ac and H3K4me1, we here show that the dual histone modification mark H3K4me1-H3K14ac is recognized by ZMYND8 (also called RACK7) and functions to counteract gene expression. We identified ZMYND8 as a transcriptional corepressor of the H3K4 demethylase JARID1D. ZMYND8 antagonizes the expression of metastasis-linked genes, and its knockdown increases the cellular invasiveness *in vitro* and *in vivo*. The plant homeodomain (PHD) and Bromodomain cassette in ZMYND8 mediates the combinatorial recognition of H3K4me1-H3K14ac and H3K4me0-H3K14ac by ZMYND8. These findings uncover an unexpected role for the signature H3K4me1-H3K14ac in attenuating gene expression and reveal a previously unknown metastasis-suppressive epigenetic mechanism in which ZMYND8's PHD-Bromo cassette couples H3K4me1-H3K14ac with downregulation of metastasis-linked genes.

34. Evolving Spindlin1 Small Molecule Inhibitors Using Protein Microarrays

Narkhyun Bae^{1*}, Monica Viviano^{2*}, Xiaonan Su^{3*}, Cari Sagum¹,

Sabrina Castellano^{2,4}, Claire Johnson¹, Mahmoud Ibrahim Khalil^{1,5},

Haitao Li^{3§}, Gianluca Sbardella^{2§} and Mark T. Bedford^{1§}

¹Department of Epigenetics and Molecular Carcinogenesis, The University of Texas MD Anderson Cancer Center, Smithville, TX 78957, USA.

²Dipartimento di Farmacia, Epigenetic Med Chem Lab, Università degli Studi di Salerno, Via Giovanni Paolo II 132, I-84084 Fisciano (SA), Italy.

³Center for Structural Biology, Department of Basic Medical Sciences, School of Medicine, Tsinghua University, Beijing 100084, China.

⁴Dipartimento di Medicina e Chirurgia, Università degli Studi di Salerno, Via Salvador Allende, I-84081 Baronissi (SA), Italy

⁵Department of Molecular Biology, Faculty of Science, Alexandria University, Egypt.

Epimutations, unlike genetic mutations, can be reversed by chemotherapeutic intervention, making epigenetic therapy conceptually extremely appealing. The recent discovery of inhibitors of methyl- and acetyl-binding domains has provided evidence for the “druggability” of epigenetic effector molecules. All known methyl-binding domains harbor an aromatic cage. The small molecule probe, UNC1215, prevents methyl-dependent protein-protein interactions by engaging the aromatic cage of MBT domains, and with lower affinity, Tudor domains. Here, we developed a library of tagged UNC1215 analogs and screened a protein domain microarray of almost a hundred methyl-lysine effector molecules to rapidly identify compounds with novel binding profiles - either improved or loosened specificity. Using this approach, we identified a compound (EML405) that acquired a novel interaction with the Tudor domain-containing protein Spindlin1 (SPIN1). Structural studies revealed that the symmetric nature of EML405 allows it to simultaneously engage two of SPIN1's Tudor domains, and also facilitated the rational synthesis of more selective SPIN1 inhibitors (EML631-3). The EML631-3 compounds engage SPIN1 in cells, block its ability to “read” H3K4me3 marks, and inhibit its transcriptional coactivator activity. Protein microarrays can thus be used as a platform to target jump and identify small molecules that bind and compete with domain – motif interactions.

35. Neuroanatomical Differences in Speech Perception Ability in Bilingual Children

Archila-Suerte, Pilar; Vasquez, David; & Hernandez, Arturo

Accurate and efficient processing of second language (L2) speech sounds has been associated with different characteristics of brain anatomy (Golestani et al., 2007, 2011). The goal of the present study was to evaluate the effect of foreign accent, age, and age of acquisition (AoA) on the anatomy of the bilateral superior temporal gyrus (STG). Spanish-English bilingual children between the ages of 6 and 10 and an AoA mean of 5 yrs participated in this study (N = 32). Participants' speech samples were recorded while reading a list of 168 English words. Their foreign accent was judged on a 9-point scale by English monolinguals. High-Resolution whole-brain T1-weighted images were acquired in a 3T Siemens scanner (192 slices, 1x1x1 voxel size, 87.5% FoV Phase). Two multiple regressions were conducted, one for each outcome variable: the left hemisphere STG and the right hemisphere STG. The predictor variables were foreign accent, age, and AoA. Results showed that in bilingual children, foreign accent predicted surface area of the bilateral STG independent of age and AoA. That is, children with native-like accents in L2 had larger surface areas of the bilateral STG, independent of the age of the child and when the child learned the L2. These results indicate that foreign accent, which significantly correlated with L2 proficiency ($r = -.66$, $p < 0.001$), better predicts the size of the STG bilaterally than actual age or AoA. It appears that abilities in speech perception, as measured by foreign accent, influence the anatomy of the STG.

36. Adrenergic signaling promotes cervical tumor growth and dissemination.

Piotr L. Dorniak¹, Justyna Filant, Archana S. Nagaraja, Nouara C. Sadaoui, Jean M. Hansen, Rebecca A. Previs, Guillermo N. Armaiz-Pena, Susan K. Lutgendorf, Steve W. Cole, Anil K. Sood.

¹ The University of Texas MD Anderson Cancer Center, Houston, TX

Cervical cancer (CvCa) is the common gynecologic malignancy that accounts for >275,000 deaths every year. Clinical and experimental evidence concordantly solidifies the role of bio-behavioral factors, such as chronic stress, depression and low social support, in promoting tumor progression. In the present study, we developed novel orthotopic mouse models of human CvCa and utilized multiple *in vitro* approaches to discover and understand effects of neuroendocrine stress mediator norepinephrine (NE) on cellular functions relevant to CvCa growth and metastasis. Nude mice were subjected to a mid-ventral laparotomy and received an injection of 10⁶ SIHA cancer cells into the uterine cervix. An orthotopic CvCa mouse model was used for restraint stress experiments. Relative to the non-stress control, restrained stress increased cervical tumor growth and metastatic tumor nodule formation, whereas co-treatment with beta-blocker propranolol attenuated stress effects on CvCa dissemination. Treatment with selective beta 2-adrenergic agonist terbutaline mimicked protective effects of NE on CvCa during anoikis and stimulated expression of a number of anti-apoptotic molecules. Silencing of expression of NE-induced pro-survival proteins in cervical tumors abrogated chronic restraint stress effects on CvCa growth and dissemination. Clinical data analyses found that high expression of ADRB2 correlates with poor overall survival of CvCa patients. Interventions blocking the adverse stress effects will provide novel therapeutic avenues for improving conventional treatments.

37. Unique molecular signatures to distinguish immunotherapy responding and resistant cell lines in melanoma

Shivanand Pudakalakattia¹, Ashvin Jaiswalb², Michael Curranb², Pratip Bhattacharyaa¹

¹Department of Cancer Systems Imaging, UT M D Anderson Cancer Center, Houston, TX

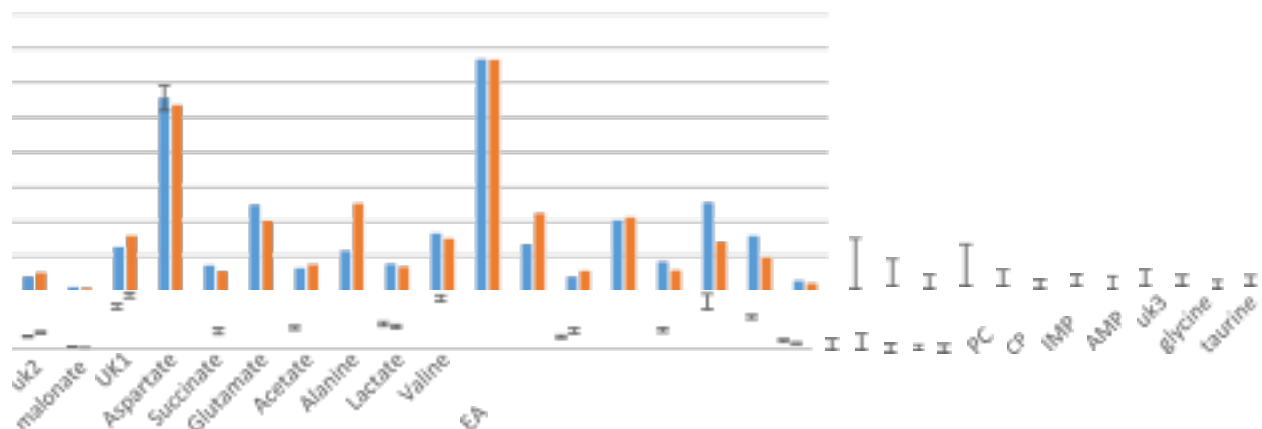
²Department of Immunology, UT M D Anderson Cancer Center, Houston, TX

Background: Cancer immunotherapy is a promising alternative to conventional therapies, including surgery, radiotherapy and chemotherapy. However, the translation of this technique to clinic is hindered due to its limited success. The different approaches to predict the immunotherapy responses of cancer to increase the success rate are under development in many laboratories. Bridging the knowledge gap of understanding the response of immunotherapy in individuals at metabolic level is the overarching goal of this investigation.

Methods: Nuclear Magnetic Resonance (NMR) Spectroscopy is used as an analytical tool to understand the metabolic responses in melanoma cancer of immunotherapy resistant and immunotherapy responding cell lines. The cell line B16/BL6 TMT is responsive to immunotherapy while B16/BL6 3I F4 is completely resistant. Both cell lines, B16/BL6 TMT (parental) and 3I-F4 (resistance) were cultured in 15 cm plate. The individual cells were collected in appropriately labeled cryo-vials and snap frozen in liquid nitrogen and stored in -80 °C refrigerator until the collection of NMR data. The standard one dimensional (1D) ¹H NMR with water suppression sequence was used to acquire the data. The data was processed in Topspin 3.1 and analyzed by Chenomx. The metabolites were identified using Chenomx, Human Metabolic Database (HMDB), 2D [¹H-¹H] TOCSY and 2D [¹H-¹³C] HSQC.

Results: The analysis of 1D ¹H NMR revealed distinct difference in metabolic activity in two different cell lines. The metabolites lactate, alanine and phosphocholine (PC) were altered significantly in the two individual cell lines (Figure 1). The lactate and alanine were overexpressed whereas phosphocholine production is suppressed in immunotherapy resistant 3I-F4 cell line.

Conclusion: This study validates our observation that altered concentration of lactate, alanine and phosphocholine are correlated to the immunotherapy resistant individuals. The study will now be extended to murine derived tumors from these two individual cell lines to identify metabolic biomarkers that can potentially be employed for MR imaging to classify patients responsive to immunotherapy. To further understand the relationship of metabolism and immunotherapy resistance in melanoma, we plan on silencing the genes responsible for the expression of lactate, PC and alanine and validating the consequent immunotherapy responses.



F4 Resistant

TMT Responding



Figure 1: Comparative bar plots of metabolites showing marked difference across two cell lines:
I) immunoresponsive, B16/BL6 TMT and II) immuno-resistant, B16/BL6 3I F4.

38. Predicting the clinical outcomes using imaging covariates with missing responses

Tengfei Li

To use the large MRI dataset together with demographic information or genetic information to do voxel-wise analysis and predict clinical outcomes, is always a hot topic and under rapid development, which initiates many statistical problems like functional statistical analysis, high dimension reduction and missing data imputation. Here we study the general scenario when responses are subject to missingness without missing-at-random assumption, under the environment of imaging functional analysis. This happens in real data usually when questionnaires or intelligence score tests have got no answer for a certain group of individuals, and this group has certain relationship with the value of the missing responses itself. We shows that these non-response subjects still contains information and ignoring them leads to non-response bias. How to make use of such information to improve the MRI prediction is our main concern. We propose an ETFLM model using which the prediction accuracy of the behavior information is highly improved in the ADNI (Alzheimer's disease Neuroimaging Initiative) dataset. We develop the corresponding Matlab GUI (software) and a pipeline for people to use it. Finally, from the ADNI dataset we get our conclusion, education, Apoe4, and Alzheimer's Disease strongly influence the individual's learning test score; people with low learning test score have the tendency to be absent to the test; brain regions like lateral ventricle and caudate nucleus have strong negative effect on learning ability.

39. Modified oncolytic adenovirus, Delta-24-RGDGREAT, as an immunotherapeutic agent for Glioblastoma

Yisel A. Rivera Molina¹, Hong Jiang¹, Candelaria Gomez-Manzano^{1,2}, and Juan Fueyo^{1,3}

¹ Department of Neuro-Oncology, The University of Texas MD Anderson Cancer Center, Houston, TX 77030, USA

² Department of Genetics, The University of Texas MD Anderson Cancer Center, Houston, TX 77030, USA

³ Department of Neurosurgery, The University of Texas MD Anderson Cancer Center, Houston, TX 77030, USA

Glioblastoma is one of the brain tumors with a median survival of 14 months and a poor prognosis. The standard methods of treatment have been based on the combination of surgery, radiotherapy and chemotherapy. Nowadays, immunotherapy has emerged as a potential treatment for brain tumor. In this project, the purpose is to use as a virotherapy, an improved version of the oncolytic adenovirus, Delta-24-RGD. This oncolytic virus has showed promising results in clinical trials. We *hypothesize* that by targeting the glioblastoma using a modified Delta-24-RGD expressing a costimulator can enhance the immune response producing an anti-tumor activity. Delta-24-RGDGREAT, which expresses a ligand from the family of the tumor necrosis factor, glucocorticoid-induced TNF receptor ligand (GITRL), can upregulated and attract more T effector cells to the tumor area. The *significance* of this study is to contribute by improving the median survival of glioblastoma patients. Our results demonstrate a median survival of more than 60% ($p < 0.0001$) after intracranial treatment of Delta-24-RGDGREAT in GL261 glioma-bearing mice. Brain infiltrated lymphocytes (BILs) increase in glioma-bearing mice after characterization of the T cell populations, CD45/CD3/CD4 and CD45/CD3/CD8, in the brain. CD45/CD3/CD8 subset was highly increased in the tumor environment after virotherapy. In addition, co-culture experiments with tumor cells infected with viruses and splenocytes isolated after treated glioma-bearing mice demonstrated a response against the tumor site. Moreover, an increment of IFN- γ was observed indicating a recruitment of CD4+ and CD8+ lymphocytes that may correlate to the anti-glioma immunity that extended the survival of mice. Survivors did not show evidence of tumor growth after re-challenging with GL261 glioma. It confirmed that an immune response has been elicited against the tumor. However, survivors of GL261 tumor did not survive a re-challenge after intracranial implantation of B16/F10 melanoma. These results showed that the immune response is specific and against glioma antigens. Taking together, our results demonstrate that modified oncolytic virus expressing a positive immunodulator may be used as an immunotherapy for the treatment of glioblastoma.

40. Spatial Large-Margin Angle-Based Classifier for Multi-Category Neuroimaging Data

Leo Yu-Feng Liu¹, Yufeng Liu¹ and Hongtu Zhu²

¹Department of Statistics and Operations Research 2Department of Biostatistics The University of North Carolina at Chapel Hill, NC

With the development of neuroimaging techniques, scientists are interested in identifying imaging biomarkers that are related to different subtypes or transitional stages of various neuropsychiatric and neurodegenerative diseases. In the literature, large margin classifiers are popular due to the flexibility in handling complex data. However, most existing methods are developed for standard classification problems. For neuroimaging classification, there are some unique challenges. In particular, the feature spaces representing the images typically have very high dimensions as well as complex spatial structure. The “off the shelf” high dimensional classifiers may yield sparse estimation, but ignore the spatial structure. On the other hand, spatial smoothing methods may improve the performance, but most existing tools are only designed for binary classification problems. In this paper, we propose a novel Fused Lasso penalized multi-category Angle-based Classifier (FLAC) for the identification of important imaging biomarkers in neuroimaging classification problems. The proposed FLAC not only utilizes the spatial structure of imaging data, but also handles both binary and multi-category classification problems. We also introduce an efficient algorithm based on an Alternative Direction Method of Multipliers (ADMM) algorithm to solve the large scale optimization problem for the FLAC. Both our simulation and real data experiments demonstrate the usefulness of the FLAC.